

Response to reviewers:

We thank both reviewers for encouraging yet constructive comments and critique. Below are point-by-point responses to their comments, along with references to line numbers for revised text in the updated version of the manuscript.

Reviewer 1

In this work the authors examine tracer dispersal due to tidal processes around the Lofoten-Vesterålen with the motivation of determining the importance of tides modulating the dispersal of cod eggs and larvae from spawning to nursery areas. They focus on two non-linear tidal processes, namely tidal pumping and tidal rectification. FVCOM is run with an unstructured grid 2D setup for tides only and subsequent tracer releases are analysed. The authors then analyse the relative importance of each process in driving the exchange of waters in and out of Vestfjorden through a number of different straits. The paper is well written, clear and nicely presented. My comments are generally related to the presentation of the results and how they could be made more easily to understand

Introduction:

L.18–21: could do with a few additional references

Good point. We have included two references on the acknowledged role of tides for vertical mixing.

Modified text in l. 19-21:

While strong tidal currents are known to cause efficient vertical mixing of the ocean, important for bringing up nutrients in the water column (e.g. Blauw et al., 2012; Richardson et al., 2000), their contribution to net horizontal transport is often underestimated due to their oscillating nature.

L 50-65: It would be nice to have a diagram to illustrate this process. You could move Figure 9 to the intro and refer to it here as it greatly adds to the intuitive understanding of the process.

L 68-83: Again, it would be nice to have the diagram for this in the intro.

This is an interesting suggestion. We have considered moving the two diagrams (Figs. 9 and 14) to the intro to help illustrating the two transport processes better. However, on further thought we decided against this since Fig. 9 contains details (definition of parameters), which, we feel does not belong in an introduction section.

So, we did not move the diagrams to the introduction. Instead, we landed on a compromise, adding references (in parentheses) to these two figures in the Introduction (l. 56 and 74).

Methods:

L 118: Why do you use TPXO7.2? The latest version is 9 and is available as a higher resolution dataset. This is likely to affect your results. By how much do open boundary forcing values differ between the two datasets?

The actual model run was conducted a few years back, but we got delayed in analyzing the data and writing this paper. This is why an older version of TPXO has been used. However, we believe that the validation against previous studies as well as observations is the most important check regarding model performance. We take the favorable comparisons shown in Figure 5 as indication that this model is adequate for investigating what are, first and foremost, qualitative aspects of the tidal dynamics and transport in the region.

Incidentally, Figure 5 has been updated after a bug was found in the validation script. The agreement is arguably better after the update except for the phase of the S2 tide (which, however, has a very small amplitude compared to other constituents).

Modified text in l. 141-144:

Furthermore, the sea surface height and phase from the model fit reasonably well with observations from five stations provided by the Norwegian Mapping Authority, Hydrographic Service (2021), as shown in Fig.5. One notable exception is the phase of the S2 tide, but the amplitude of this is very small compared to the other constituents.

Model validation:

It would be nice to see some numerical values so that the reader can assess the performance of the model in absolute terms. Could you add a table with the amplitudes, phases, and amplitude and phase errors for each station for M2 and K1? You could also report mean errors for each constituent analysed.

We have included two new tables (Tables 1 and 2) with the values from M2 and K1, corresponding to Fig. 5. In these tables we have also included the 95% confidence interval for the sea surface height amplitude, but not for the current meter data since these statistics are not given in Moe et al 2002.

Tidally driven transport:

L.177: Why do you show results only for 3 and 4.5 hours? It would be good to see the process through the tidal cycle at e.g. hourly intervals.

We agree that a higher temporal resolution could be useful in these figures. However, there needs to be a compromise. Essentially, including many more time-steps will make each subfigure smaller and harder for the reader to interpret. The figures show that dipoles form and partly escape the return flow in these two straits, which is the main point. We landed on a compromise of adding two subplots, showing the situation additionally at 1.5 and 7.5 hours (after the first slack tide).

Modified text in caption, Figure 7:

The two upper panels and the left middle panel are during northward flow (flood tide), and the right middle panel and the two lower panels are during southward flow (ebb tide).

Modified text in l. 173-176:

The various panels show the situation at various times after slack tide after ebb tide. So, the first three panels (1.5, 3 and 4.5 hours) show conditions during the flood tide while the last three (7.5, 9 and 10.5 hours) show conditions through the following ebb. Already at 1.5 hours after slack tide we

see that the northward-flowing tidal current has separated from the coast near the abrupt opening in the north.

Modified text in l. 178:

The vortices form a self-propagating dipole pair and grow in time, as can be seen at 3 hours and 4.5 hours.

Modified text in l. 181:

The ebb tide (7.5, 9 and 10.5 hours in the Fig. \ref{fig: Nappstraumen}) returns water to the northern opening as potential flow, following the shape of the coastline.

Modified text in l. 190-193:

A closer inspection shows that the dipoles form later in the tidal cycle compared to the generation at the northern exit in Nappstraumen (3 hours compared to 1.5 hours),

Rectified tidal transports:

L.335: I'm not sure this sentence fully makes sense? Which mechanism dominates and is responsible for the net flux or how does each process contribute?

We agree with you here and have modified the text here in the revised manuscript. The main message that we try to get across is that tidal pumping is the dominating mechanism causing net fluxes out of Vestfjorden in general. But south of Røst the net flux is mainly due to tracer advection by the rectified tidal currents (not tidal pumping).

Modified text in l. 330-333:

So even though much of the net tracer transport south of Lofotodden is due the tidal pumping mechanism investigated above, there is also a contribution driven by anticyclonic mean flows around the islands here. This mechanism appears to be particularly important south of Røst where, it should be noted, there can be no formation of self-propagating dipoles

L343: How will your choice of linear bottom friction impact your results? Is this the same bottom friction used in the tide model? It may be an issue if they are not consistent?

The numerical model uses quadratic bottom friction whereas in our discussion of theory we have used linear bottom friction in order to arrive at closed-form analytical expressions (eqns. 12 and 13).

As for comparison between simplified theory and numerical results (with regards to the response to the spring-neap cycle), we primarily seek an order-of-magnitude agreement since the theoretical expression is obviously simplified. The reviewer's comments nevertheless led us to improve on our previous estimate for an effective linear drag coefficient. Essentially, we set $R = C_d * |u|$, where C_d is the model's quadratic drag coefficient and $|u|$ is an expected magnitude of current strength.

As outlined in the text, we investigated 5 and 9 closed depth contours around Mosken-Værøy and around Røst, respectively. Updating these calculations, now using the model's actual drag

coefficient ($C_d= 0.0025$) and mean values for current strength $|u|$ (0.29 and 0.23 m/s for Mosken/Værøy and Røst, respectively), led to an updated Figure 13.

Here, we found effective linear friction coefficients to be $R = 8.6 \cdot 10^{-4} \text{ m/s}$ and $R = 5.7 \cdot 10^{-4} \text{ m/s}$, for Mosken/Værøy and Røst, respectively. These are mean value for all the closed depth contours around each of the island groups. Using these updated values in our expression for phase lag,

$$\phi = \tan^{-1} \left(\frac{\omega_{sn} H}{R} \right),$$

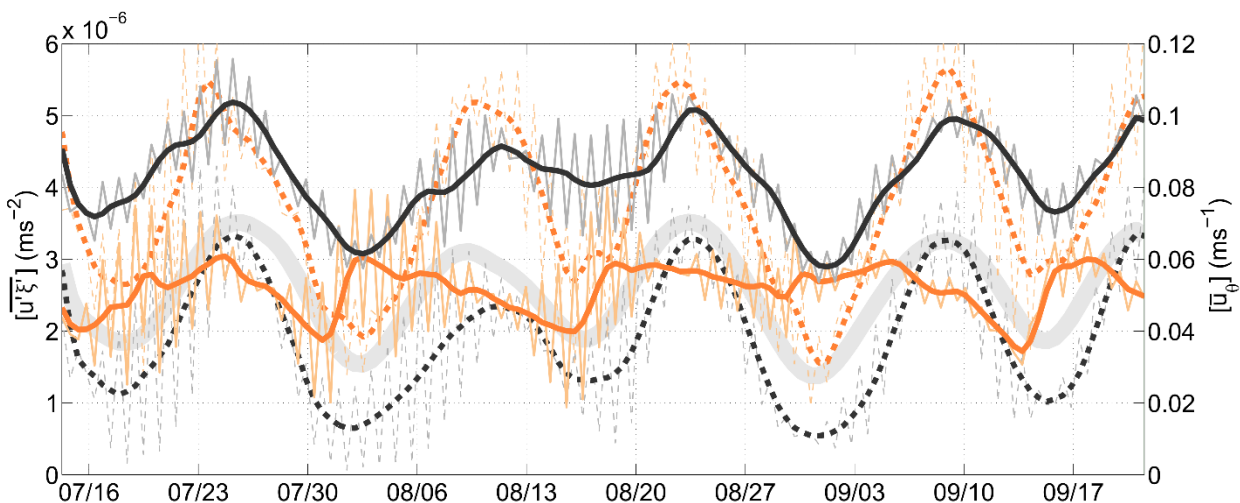
we obtain an updated mean phase-lag of the response to the spring-neap cycle of 0.6 days (0.24 rad/s) and 0.9 days (0.39rad/s), for Mosken-Værøy and for Røst, respectively.

Modified text in l. 367-374:

The primary slow time scale variation in forcing for our problem is the spring-neap cycle. So $\omega_{sn}= 2\pi/14.75 \text{ rad days}^{-1}$. To test the theory with respect to this variation we additionally need to specify a depth level H and a linear friction coefficient R . Our FVCOM model uses quadratic bottom drag, but an equivalent linear drag coefficient can be found from $R=C_d|u|$, where $C_d= 0.0025$ (the value used in the model) and $|u|$ is a typical current strength. We diagnosed values of 0.29 and 0.23 m s^{-1} for the current strength around Mosken-Værøy and Røst, respectively, and used these to calculate equivalent linear friction coefficients. Then taking a typical depth where the slope is steep, $H = 50\text{m}$, we calculate theoretical spin-up times of approximately 21 and 14 hours which corresponds to a phase lag ϕ of about 0.39 and 0.24 radians, for Mosken-Værøy and Røst, respectively.

L375: How does the choice of filter impact the curves? It would be nice to see 1 tidal cycle values as well.

The purpose of the low-pass filter is to make the figure cleaner by removing the dominating diurnal and semi-diurnal variations. But we found that it was possible to add these with thinner lines—and updated Figure 13 accordingly (reproduced below).



L440: I'm not sure I understand how you define the topographic length scale

L445: Where do you define L_B and what is it? How does it differ from L ?

We see that we have forgotten to define the topographic length scale in the manuscript and thank the referee for pointing this out.

L_B is the topographic length scale, defined as follows:

$$L_B = \frac{H_0}{\alpha}, L_B = \frac{H_0}{\Delta H}$$

where H_0 is a mean depth and $\alpha = \Delta H$ is the slope of the bottom topography. L_B is thus used to characterize bathymetric feature, which will cause water to move vertically over a ridge or a bump etc. at the sea floor bottom. L on the other hand is the horizontal distance the water column has moved within some time dictated by a given dynamical process. In our case here, $L = L_T$, where L_T is half a tidal cycle.

We have now included the definition of topographic length scale in the manuscript in lines 446-47: A topographic length scale $L_b = H_0/\Delta H$ can then be defined as that which gives a depth excursion equal to the initial depth, or $H_0 = \alpha L_b$.

Summary and conclusion:

L.492: 'But not all straits are created equal' – reword to something more specific.

This was a play on words inspired by wording in the American Declaration of Independence. We have reworded this general transitional sentence, but we leave specifics to the sentences that complete that paragraph.

Modified text in l. 499-500:

But geometry and flow conditions around each strait are different, and the tracer transport due to tidal pumping varies greatly.

General: Given that your introduction talks about cod quite a lot, the reader feels a little let down in the conclusions. How important are these tidal processes for the dispersal of the Arctic cod?

This is a good point. Since we only investigate purely tidally driven flows in this manuscript, we cannot say too much about the contribution relative to other processes that impact the drift of cod eggs out of Vestfjorden (winds, background currents, freshwater run off etc.). For such an assessment we point towards our more complete 3D follow-up study at the very end of the Conclusions section. But, to not promise more than we can keep in this manuscript, we have now downplayed the focus on cod-eggs in the introduction.

Modified (shortened) text in l. 24-29:

In this study, we will investigate nonlinear tidal dynamics around Lofoten-Vesterålen in Northern Norway (Fig. 1), a major spawning ground for the Northeast Arctic cod (Hjermann et al., 2007). Spawning of this species takes place all along the middle and northern Norwegian coast, but as much as 40 percent of the cod spawns in Vestfjorden southeast of the Lofoten-Vesterålen archipelago (Ellertsen et al., 1981; Sundby and Bratland, 1987). Therefore, a good understanding of ocean dynamics controlling the drift and spreading patterns of biogeochemical material, and cod eggs and larvae in particular, is important for identifying particularly vulnerable regions and factors controlling the recruitment of the Northeast Arctic cod.

How do the observed processes compare to other regions in the world and different observations? It would be nice to see this work be put into context of other previous work in this section.

This is a useful suggestion. We have now put the work a bit more into context of previous work in the revised manuscript, mainly in the Conclusions section.

Modified text related to tidal pumping in l. 504-511:

Tidal pumping, particularly in relation to tidal flushing of estuaries and near-shore regions, have been widely studied elsewhere. Certainly, the formation of dipole vortices is observed many places where prominent tidal currents exit narrow straits, for example in Aransas Pass (USA), Messina Strait (Italy) and the Great Barrier Reef (Australia) (Whilden et al., 2014; Cucco et al., 2016; Delandmeter et al., 2017). Cucco et al. (2016) show that the strong tidal currents and subsequent pumping is important for water exchange and for modifying the thermohaline properties in two large sub-basins of the Western Mediterranean Sea. We thus consider it possible that tidal pumping in Lofoten and Vesterålen not only contributes to transport of dynamically passive particles such as cod eggs but is also important for the transport of freshwater out of the large Vestfjorden embayment, thereby modifying the thermohaline properties here.

Modified text related to tidal rectification in l. 522-527:

We find that the potential for tidal rectification can be evaluated through the relation L_T/L_B , where values near one indicate prominent rectification (Loder, 1980). The residual currents around the island groups in southern Lofoten thus appear to be governed by dynamics similar to what is observed around Georges bank (Loder, 1980; Limeburner and Beardsley, 1996; Chenet et al., 2001). There, the residual currents encircling the bank in a clockwise fashion are of similar strength as the flow we model around Røst and Mosken/Værøy (0.2–0.3 m/s). Using the values provided in table 1 in Loder (1980), we find that on the northwestern and northern side of Georges Bank $L_T/L_B \sim 1$, equivalent to what we find for the islands of southern Lofoten.

Figures:

Here we will only shortly comment on the direct questions. Suggestions of technical improvements and rephrasing figure captions have all been implemented in the revised manuscript.

Figure 2: It would be nice to have more information with this figure: e.g. (a) how do the two figures differ? (I guess it's the phase of the tide); (b) the velocity front is identified – why is this relevant and what does it mean for this study?

The purpose of this figure is to show that formation dipoles and tidal jet are actually observed in Moskstraumen, and not merely a result of numerical modelling. But we have added some information to guide the reader.

The caption now reads:

Satellite images from Copernicus Sentinel-II missions, tracing out surface currents in Moskstraumen and Nordlandsflaget. The left panel shows the current structure during westward flow (during flood tide); west of Lofotodden a velocity front is evident which is likely related to dipole formation. The right panel shows the current structure during eastward flow; here, a dipole east of the strait with a trailing jet is evident. The Sentinel-II missions satellites carry a multi-spectral instrument with 13 spectral channels in the short-wave infrared and visible/near infrared spectral range,

whereas this image is collected from band B4 (664.6 nm). The satellite imagery was assessed and processes using data from the Norwegian National Ground Segment for Sentinel data (Halsne et al., 2019, pers. comm. Trygve Halsne).

Figure 4: how about plotting observed values on top as shaded circles on top of the model results? Also, plot against latitude and longitude rather than distance.

The suggestion of plotting observed values on top of the model results is a good idea. However, the observations are typically located near land, e.g. inside straits, where gradients are large. We thus decided against adding observations in this figure, both because adding shaded circles would make the figure messy and potentially hide the overall structure of the tides, and because model-observation comparisons are presented in Fig. 5 and (new) Tables 1 and 2.

We have plotted against latitude and longitude but did not add observations to the figure.

Figure 6, l.5: do = does

Fixed.

Figure 7: Could you take your panels a bit further south? At 10.5 hours you are missing part of the incoming waters

We eventually decided against this since the water is flowing out of the southern opening at 10.5 hours. The textual focus here is on the dipole on the northern side.

Figure 9: Panel b: Why is A_e in the sink region? Should it not be in the jet? It would be nice to illustrate all of the length scales on this plot (as far as possible)

A_e is in the jet (the black two-headed arrow). But we see that the location of the label was poorly placed.

We have now moved the label further south and included an arrow showing the sink radius.

Figure 10: Not all marker labels are visible. Also, you could increase the intuitiveness of the plot by adding labels such as an arrow with 'more asymmetric' along the axis y axis and doing the same for the x-axis.

We have adjusted labels so that they are now all visible. We have also added 'help' arrows, as suggested.

Figure 11: Mention what each non-dimensional parameter is in words either on the axis or in the legend.

Done. The new caption is now:

The tracer transport efficiency T_p^ plotted against non-dimensional parameters (a) Ax_0 , representing flow asymmetry, (b) L^* representing strait length and (c) Ax_0L^* , combining the two non-dimensional parameters. Two estimates of Ax_0 are shown for Gimsøystraumen (5).*

Figure 13: What do you mean by 'sets of closed contours'? Could you show these on a map?

The "sets of closed contours" should have been phrased as "sets of 5-9 closed depth contours encircling the island groups". We have now included a map similar to the one in Figure 17 for the readers to see the locations of these contours.

Figure 14: It would be nice to add the positive/negative vorticity gains in the diagram – it would make it even more intuitive. You could also explicitly include the words squeezing and stretching in the diagram.

The figure has now been modified according to these suggestions.

Minor comments:

Generally, watch out for the use of commas. E.g. Here, ... In this study,...

l.16: rises = raises

l.54: is = are

59: what = which

102: no comma needed

425: 'is down the' = is down to the

520: appears = appear

Thanks. We have edited the manuscript according to all of the comments, and a check of comma use has been done.

Reviewer 2

This paper discusses two physical processes, tidal pumping and tidal rectification, that may be relevant to the dispersion and transport of cod eggs and larvae in the Lofoten - Vesteralen area, Northern Norway.

The geographical and ecological settings, as well as the physical processes and numerical techniques used to address the questions involved in larvae and cod egg transport and spreading are well described. The paper comes to a clear conclusion regarding the relevance of tidal pumping, and provides welcome suggestions for further investigation of the process of tidal rectification.

As a consequence, it is recommended that the paper is published provided it addresses the few minor issues discussed next.

Line 404: The along-isobath velocity scale U may be much stronger than the cross-isobath current used in the previous scaling (line 403).

Good point. The amount of asymmetry between the two velocity components (along and across topography) will depend on both time and length scales of the problem. For high-frequency tidal oscillations the cross-isobath component need not be severely constrained (as it will be e.g. for subinertial, geostrophic flows), but some asymmetry is likely to be found. We actually looked into the model and found the ratio between along- and across-slope velocity components around the island groups to be 1.2–1.4.

We have included a small discussion on this in l. 409-415:

Comparing the magnitude of the two terms, using typical values for Mosken-Værøy and Røst as above ($D \sim 50$ m, $R = 6 \cdot 10^{-4}$ and $9 \cdot 10^{-4}$ m s⁻¹ and $f \sim 10^{-4}$ s⁻¹), gives $fD/R \sim 6$ and 12 for Mosken-Værøy and Røst, respectively. Here, we have picked a depth value which corresponds to the steeper parts of the slope (where vorticity generation by either mechanism can be assumed to be most relevant) and assumed that the along-slope and cross-slope velocity components are of similar magnitude. One might intuitively expect the along-slope component to be larger than the across-slope component, but perhaps primarily for longer-timescale (subinertial) motions. Diagnosing the model fields around Mosken-Værøy and Røst showed that the ratio between the two is only about 1.2–1.4 for the tidal motions considered here (calculated for the depth contours in Fig. 13). This suggests that vorticity production by flow up and down topography is quite a bit larger than production by bottom friction torque.

How is the value of R motivated?

In the original manuscript we used a literature value for the linear drag coefficient. However, in response to comments from both reviewers, we have updated the calculations in the manuscript using an effective linear friction coefficients $R = Cd * |u|$ instead, where Cd is the model's quadratic drag coefficient and $|u|$ is an expected magnitude of current strength. By using the model's actual drag coefficient ($Cd = 0.0025$) and mean values for current strength $|u|$ (0.29 and 0.23 m/s for Mosken/Værøy and Røst, respectively), we obtain effective linear friction coefficients of values $R = 8.6 \cdot 10^{-4}$ m/s and $R = 5.7 \cdot 10^{-4}$ m/s for Mosken/Værøy and Røst, respectively. These are mean values calculated for 5 and 9 closed depth contours between 30 m and 50 m around Mosken/Værøy and between 30 m and 70 m around Røst, respectively.

Modified text in l. 367-374:

The primary slow time scale variation in forcing for our problem is the spring-neap cycle. So $\omega_{sn} = 2\pi/14.75$ rad days⁻¹. To test the theory with respect to this variation we additionally need to specify a depth level H and a linear friction coefficient R . Our FVCOM model uses quadratic bottom drag, but an equivalent linear drag coefficient can be found from $R = Cd|u|$, where $Cd = 0.0025$ (the value used in the model) and $|u|$ is a typical current strength. We diagnosed values of 0.29 and 0.23 m s⁻¹ for the current strength around Mosken-Værøy and Røst, respectively, and used these to calculate equivalent linear friction coefficients. Then taking a typical depth where the slope is steep, $H = 50$ m, we calculate theoretical spin-up times of approximately 21 and 14 hours which corresponds to a phase lag ϕ of about 0.39 and 0.24 radians, for Mosken-Værøy and Røst, respectively.

Closer to islands, D decreases. So, how appropriate is a choice $D = 50$ m?

In Figure 1 below, we show a spatial calculation of fD/R . Here we used an effective linear friction coefficient $R = Cd * |u|$, where $|u|$ is the amplitude of current speed, independent of direction (as outlined in our response to the previous comment). At very shallow depths, less than 20-30 m, the bottom friction torque begins to dominate. However, here the slope (inclination) is generally gentle, and vorticity generation is expected to be weak. The steeper parts of the slope, where we expect the main vorticity generation to occur, by either mechanism, is mainly located between 30 and 100 m (seen from the bottom contours). These depths are therefore the most interesting to investigate regarding vorticity generation and rectification (compare with Fig. 12 of the manuscript). Therefore, we believe that 50 m is a reasonable choice for the scaling, and that vorticity generation by squeezing and stretching dominates in general around these slopes. But,

fD/R is not much greater than one over the slopes; hence, we do not believe the bottom friction torque is negligible—as we already state in the manuscript.

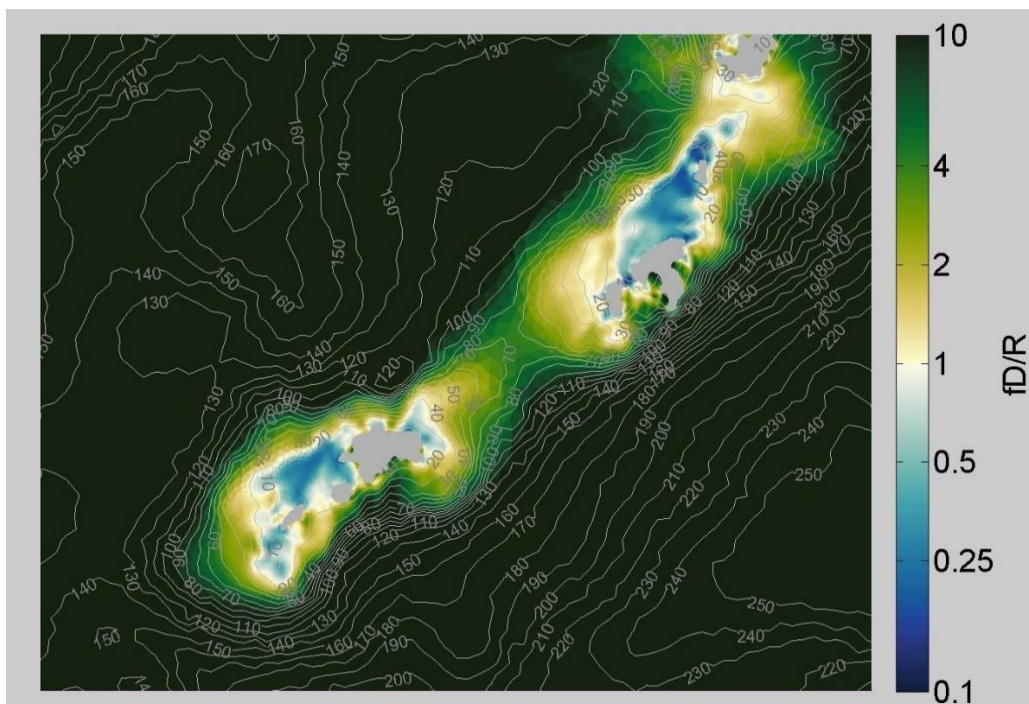


Figure 1 Estimates of fD/R for the region around Mosken/Værøy and Røst. Contours show the bottom topography.

We have included a small comment on this point in l. 409-415 (same text as for comment on anisotropic velocities above).

Line 519: Bottom intensification of tidally rectified flows and concomitant vertical circulation cells (Maas et al 1989) might possibly be of relevance for the transport and spreading of marginally sinking larvae and cod eggs.

Thank you for the reference. Another related issue: the prominent tidal motion, particularly in interaction with topography, will also induce strong vertical mixing which may greatly reduce the stratification. So, the amount of bottom intensification is presumably influenced by small-scale mixing processes set up by the same currents that drive the mean flow. As mentioned in the manuscript, we intend to have a look at stratification effects in the 3D follow-up study and assessing bottom intensification would be a natural part of that.

The Maas and Zimmermann (1989) reference has been included in a general listing of possible 3D effects, in l. 544-549:

Our simulations were also limited by their 2D nature. A 2D configuration was chosen to help isolate nonlinear lateral tidal dynamics, but the model was thus unable to account for baroclinic effects. Such effects include the generation of hydraulic jumps and vertical mixing around strait openings (Lyngé et al., 2010), the establishment of density fronts around the rectification cells (Ou, 2000) and also bottom intensification of such rectified flows, with concomitant vertical circulation cells around banks and islands (Maas and Zimmerman, 1989; White et al., 2005, 2007). So, in reality, baroclinic flow dynamics will also impact tracer transport, both vertically and laterally.

Figures A1 and A2 have interchanged captions

Yes, thank you for pointing this out. We have now fixed this.

Line 53: waters => water

Caption Fig. 2: instruments => instrument

Line 127: drop 'the'

Line 443: chances => changes

Line 462: dynamically => dynamical

Line 519: Bottom intensification of tidally-

We have fixed all these mistakes in the revised manuscript.